SIMULTANEOUS WIND AND RAIN RETRIEVAL USING SEAWINDS DATA

David W. Draper and David G. Long
Brigham Young University, MERS Laboratory: 459 CB, Provo, UT 84602
801-422-4884, FAX: 801-378-6586, draperd@et.byu.edu

Abstract

The SeaWinds scatterometer is designed primarily to retrieve winds over the ocean. Since the deployment of SeaWinds on QuikSCAT in 1999, rain corruption in wind measurements has been recognized as one of the largest contributers to wind retrieval error. This paper presents a new estimation method that incorporates rain effects into SeaWinds wind retrieval. The new method simultaneously retrieves wind and rain, giving improved wind estimates in rain-corrupted areas and providing SeaWinds-derived estimates of the rain rate. The simultaneous wind/rain estimation method works especially well in the "sweet spot" of SeaWinds' swath. On the outer-beam edges of the swath, rain estimation is not possible. This area, however, is only a small fraction of the total data. Wind speeds from simultaneous wind/rain retrieval are nearly unbiased, while the wind-only wind speeds become increasingly biased with rain rate. A synoptic example demonstrates that the new method has the capability of visually reducing the error due to rain while producing a consistent (yet somewhat noisy) estimate of the rain rate.

1 INTRODUCTION

The SeaWinds scatterometers aboard QuikSCAT, launched in mid 1999, and ADEOS II, launched in November 2002, provide a unique and valuable source for wide-spread observation of near-surface ocean winds. The SeaWinds rotating pencil beam design enables wider coverage than previous fan-beam instruments including the SEASAT scatterometer (SASS), and the NASA scatterometer (NSCAT).[1] The SeaWinds scatterometer operates at high accuracy in most wind and weather conditions.

SeaWinds scatterometer wind estimation is possible due to the relationship between the near-surface vector wind and the normalized radar backscattering cross-section (σ°) of the ocean surface. This relationship has been empirically determined and is known as the Geophysical Model Function (GMF). The GMF is a function of wind speed and direction, relative azimuth angle, incidence angle, polarization and frequency. Wind estimates are formed by inverting the GMF given several σ° values from different azimuth angles.[2]

During rain (about 4 percent of SeaWinds data), the scatterometer σ° values are augmented by additional backscatter from both atmospheric rain and surface rain perturbations. The returned signal from the wind-roughened seas is also attenuated by falling hydrometeors. Because the GMF does not account for rain affects, additional scattering from rain causes estimated wind speeds to appear higher than expected.[3] Also, the directions of rain-corrupted wind vectors generally point cross-swath, regardless of the true wind.

The degradation of SeaWinds on QuikSCAT scatterometer accuracy during rain prompted the Jet Propulsion Laboratory (JPL) to develop a probability-based rain flag given several rain-sensitive parameters.[4] The JPL approach is known as the Multi-dimensional Histogram (MUDH) rain flag. Besides the MUDH flag, a variety of other rain flags for SeaWinds on QuikSCAT have been suggested, but no formal attempt has been made to correct rain-corrupted wind vectors.

This paper discusses two approaches to correct for rain-contamination. First, if an initial estimate of the rain rate is not available, simultaneous wind and rain retrieval can be performed by inverting a modified GMF that includes both wind and rain parameters. Second, given *a priori* knowledge of the rain rate, a Beysian technique can be used to provide a more accurate wind estimate. This method is advantageous for where collocated rain rates are available such as with the AMSR radiometer aboard ADEOS II. This paper uses simulation to give a "best case" scenario of *a priori* rain rate knowledge. In addition, validation studies are performed with data from the Rainfall Measuring Mission (TRMM) precipitation radar (PR). A synoptic example is then given, demonstrating the utility of simultaneous wind/rain retrieval. This paper demonstrates that it is possible to both correct for rain contamination in many cases and estimate rain using SeaWinds scatterometer data.

2 DATA

The main backscattering mechanism at scatterometer incidence angles is Bragg resonance from waves on the order of the electromagnetic wavelength (a few centimeters for SeaWinds). The size of the centimeter-scale capillary waves are in large part driven by wind stress on the surface of the water. The backscatter is a function of the magnitude and orientation of the waves, and is thus a function of the vector wind stress. Given neutral stabil-

ity conditions (equal surface air and surface temperature with an adiabatic lapse rate), the backscatter is also related to the wind at a given reference height (traditionally 10 or 19.5 meters). The relationship between the neutral stability wind velocity and σ° is known as the GMF.[5]

Because the GMF maps two parameters (speed and direction) to one (σ°), a single backscatter measurement does not represent a unique wind vector. Thus, retrieving both wind speeds and directions over the ocean requires multiple σ° measurements from various azimuth angles. The SeaWinds antenna is designed with 2 offset-feed beams: an inner h-pol beam with incidence angle of approximately 46°, and an outer v-pol beam with an incidence angle of 54°. The SeaWinds rotating antenna design achieves the needed azimuthal diversity by measuring each point on the surface at least four times, twice by each beam fore and aft as the antenna rotates. The satellite swath is segmented into approximately 25 km square wind vector cells (wvc). The measurements that correspond to each wind vector cell are combined to create a wind vector estimate.[1]

Due to the scanning pencil beam design, measurement geometry varies along the cross track. In the center of the swath (nadir region), the fore and aft beams are nearly 180 degrees apart, while the difference in azimuth between fore and aft beams go to zero on the swath edges. Also, the outer 8 wvcs on either side of the swath only obtain measurements from the outer v-pol beam. Thus, the swath edges and nadir regions have somewhat poor viewing geometry. In the off-nadir inner-beam regions (known as the sweet spots), the azimuthal diversity is very well suited for wind retrieval.[6]

Estimating wind speed and direction involves inverting the GMF given the collocated σ° measurements at each wvc. The GMF inversion method adopted for SeaWinds is a Maximum Likelihood Estimation (MLE) technique. Assuming Gaussian noise model, the probability of the retrieved measurements given the wind is

$$p(\sigma^\circ|\mathbf{u}) = \prod_i \frac{1}{\sqrt{2\pi}\varsigma_i} \exp\left\{-\frac{1}{2}\frac{(\sigma_i^\circ - \mathcal{M}(u,\chi,...))^2}{\varsigma_i^2}\right\} \quad (1)$$

where ς_i^2 is the variance on the estimated measurement, $\mathcal{M}$ is the model function, $\mathbf{u} = \{u, \theta\}$ is the wind speed and direction, and $\chi = \theta - \phi$ is the relative azimuth angle of the wind with ϕ the azimuth angle of the instrument. Wind vector solutions are estimated by finding the local maxima of eq. 1.

The noise model is a combination of uncertainty in the GMF, signal noise due to fading and thermal noise. Theoretically, the variance is defined in terms of K_{pm}, the normalized standard deviation of the GMF, and K_{pc}, the normalized standard deviation of the communication or signal noise. K_{pc} is given in terms of a quadratic function of the backscatter,

$$K_{pc} = \sqrt{\alpha + \frac{\beta}{\sigma_t} + \frac{\gamma}{\sigma_t^2}}. \quad (2)$$

where the coefficients α, β and γ depend on fading characteristics of the surface scatterers, and the signal to noise ratio (SNR) at the receiver. Also, σ_t is the true σ° without communication noise. A derivation of the variance gives,[7,8]

$$\varsigma^2(\mathbf{u}) \cong [(1+\alpha)K_{pm}^2 + \alpha]\mathcal{M}^2(\mathbf{u}) + \beta\mathcal{M}(\mathbf{u}) + \gamma. \quad (3)$$

The SeaWinds data processing uses a simplified likelihood function by dropping the outside variance term of eq. (1) and taking the logarithm,

$$l(\sigma^\circ|\mathbf{u}) = -\sum_i \frac{(\sigma_i^\circ - \mathcal{M}(u,\chi,...))^2}{\varsigma_i(\mathbf{u})^2}. \quad (4)$$

Because of symmetry in the GMF and uncertainty in the estimate, the likelihood function generally has 1 to 4 local maxima, each corresponding to a possible wind vector solution. The local maxima are known as ambiguities. After generating the set of ambiguities at each wvc, an ambiguity selection routine is required to produce a unique wind vector field. The traditional approach requires two steps: nudging and median filtering. Nudging sets each wvc to the ambiguity closest to an outside estimate of the wind. Median filtering iteratively selects the ambiguity at each wvc that most closely matches the flow of the surrounding selected wind. The median filter is repeated until convergence is reached.[9]

3 METHODOLOGY

The wind estimation process described in Section 2 inherently assumes that the effects from unmodeled factors such as salinity, sea and air temperature, sea foam, and rain are small. To account for these unknowns, the variability is incorporated into the GMF variance term K_{pm}. Rain effects, however have been shown to be appreciable, and at times dominating.[10,3]

The effect of rain on σ° can be parameterized by the additional scattering and attenuation of the signal,

$$\sigma_m = \sigma_w \alpha_{attn} + \sigma_{eff} \quad (5)$$

where σ_m is the measured backscatter, σ_w is the component of the backscatter due to wind, α_{attn} is the two-way atmospheric attenuation factor, and σ_{eff} is the effective rain scattering due to surface perturbations and atmospheric scattering. If the effects of rain are assumed to be isotropic, the parameters α_{attn} and σ_{eff} can be written as a function of rain rate. Here, we adopt a quadratic log-log model for α_{attn} and σ_{eff}.[10]

The simple rain-σ° model of eq. (5) can be used in conjunction with the GMF to create a combined rain/wind model of the form

$$\mathcal{M}_r(u,\chi,R,...) = \mathcal{M}(u,\chi,...)\alpha_{attn}(R) + \sigma_{eff}(R) \tag{6}$$

where R is the rain rate. If R is known for each measurement eq. (6) can be used to directly adjust the model values in the estimation process. When R is unknown, eq. (6) can be used to simultaneously retrieve the wind and rain.

3.1 Noise Model

Applying an MLE technique to the combined wind and rain problem requires the development of a model for the noise. The noise is assumed to be Gaussian white like the non-raining noise model. Also, the communication noise coefficients α, β and γ are assumed to not change under raining conditions.

The noise model is derived using an additional noise term K_{pe}, which is the normalized variance of the effective rain backscatter. After some simplifying assumptions, the Gaussian noise model of the combined wind/rain GMF given in Eq. 6 has the following mean and variance:

$$\mathrm{E}\{\sigma_m\} = \mathcal{M}\alpha_{attn} + \sigma_{eff} = \mathcal{M}_r \tag{7}$$

$$\begin{aligned}\mathrm{Var}\{\sigma_m\} \;\cong\; & (\mathcal{M}\alpha_{attn}K_{pm} + \sigma_{eff}K_{pe})^2(1+\alpha) \\ & +\alpha\mathcal{M}_r^2 + \beta\mathcal{M}_r + \gamma. \end{aligned} \tag{8}$$

It is interesting to note that if $K_{pe} = K_{pm}$, the form of eq. (8) reduces to the form of the non-raining variance as intuition suggests,

$$\mathrm{Var}\{\sigma_m\} \cong [(1+\alpha)K_{pm}^2 + \alpha]\mathcal{M}_r^2(\mathbf{u}) + \beta\mathcal{M}_r(\mathbf{u}) + \gamma.$$

The constant value of $K_{pe} = 0.22$ is determined to perform the best in a rain detection study. The value of the wind model standard deviation is $K_{pe} = 0.16$ which is also used in standard SeaWinds processing.

3.2 Wind/Rain Retrieval

Now that the mean and variance of the combined rain/wind backscatter have been developed, the MLE likelihood function is written as

$$l_r(\sigma^\circ|\mathbf{u},R) = -\sum_i \frac{(\sigma_i^\circ - \mathcal{M}_r(u,\chi,R,...))^2}{\varsigma_{ri}(u,\chi,R)^2}. \tag{9}$$

where $\varsigma_{ri}(u,\chi,R)$ is the variance from Eq. 8. Simultaneous wind and rain estimates are found by maximizing the likelihood function for $\mathbf{u}$, R given the backscatter values.

Like the non-raining case, the likelihood function has several local maxima corresponding to possible rain/wind ambiguities. To yield a unique wind vector field, ambiguity selection is performed. In order to conform to the no-rain method as much as possible, a nudging/median filtering ambiguity selection routine is implemented. For simplicity, nudging for the combined rain/wind retrieval is not thresholded; all ambiguities are used. Median filtering is performed using a modified vector-median filter,

$$n = \underset{i}{\mathrm{argmin}} \sum_j ||\mathbf{u}_i - \mathbf{u}_j|| \tag{10}$$

where i indexes the ambiguities at a given wvc, and j indexes the surrounding 7×7 wvc region of selected wind vector. The norm $||\cdot||$ represents the l2 (vector) norm. Thus, the median filter selects the ambiguity that minimizes the sum of vector errors between it an the surrounding selected wvcs.

A directional norm is often used in the median filter. The directional norm has been shown to work exceptionally well for wind-only retrieval,[9] because all of the wind speeds for the ambiguities are on the same order. However, for combined wind/rain retrieval, the wind speeds of the ambiguities for a single wvc are not necessarily on the same order, and thus, a vector norm is more appropriate.

4 WVC FILLING

Because of the simplicity of the rain/wind model, the rain rate corresponding to the selected local maximum of the likelihood function cannot be interpreted as the true average rain rate over the wvc. Because of the relatively high spatial variability of rain, both beam filling and wvc filling effects are significant over the 25 km wvc. For each measurement, the antenna beam response function weights the backscatter values received from the atmospheric and surface rain scatterers. Thus, depending on the distribution of the rain within the measurement, the backscatter response is altered. Additionally, the layout of the measurements, with the associated overlap and possible lack of coverage gives an irregularly-weighted rain rate estimate.

To evaluate the effect of the wvc filling, we use data from the Precipitation Radar (PR) aboard the Tropical Rainfall Measuring Mission (TRMM) satellite. The TRMM/SeaWinds collocation set includes 100 collocations from three months of data including September through November 1999 over mostly the tropics. The TRMM PR obtains measurements at a much higher resolution than SeaWinds scatterometer (about 4 km), affording an excellent data set for analysis of wvc-filling effects.

Wvc-filling deals with the difference between the effective rain rate seen by SeaWinds (a weighted rain rate

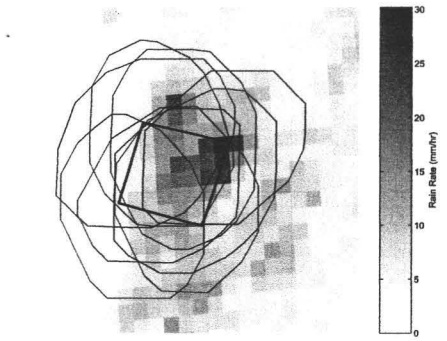

Figure 1: *The geometry of a sample wvc (bold lines) versus the layout of the actual measurements (ellipses) comprising the wvc. A PR-derived rain map is shown in the background.*

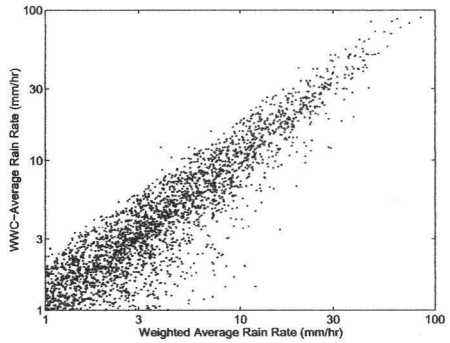

Figure 2: *The wvc-averaged (unweighted) rain rate versus the weighted average rain rate as seen by SeaWinds.*

average determined by the antenna pattern and layout of the measurements), compared with the non-weighted average rain rate over the wvc. To facilitate a comparison, we obtain a wvc-averaged non-weighted rain rate estimate, R_{nw}^{wvc} by averaging the PR-derived rain rates over each 25x25 km wvc. The wvc-averaged rain rate is compared with the "effective" weighted averaged rain rates as seen by SeaWinds. The weighted averaged rain rate R_w^{wvc} is determined by antenna-pattern-weighted averaging the PR rain rates for each measurement, and then averaging of all measurements in each wvc. A sample difference in geometry for the wvc-averaged rain rate, and the weighted averaged rain rate is displayed in Figure 1. A scatter plot of the wvc-averaged rain rates and the weighted average rain rate is displayed in Figure 2. The statistics of the normalized error defined as $(R_w^{wvc} - R_{nw}^{wvc})/R_{nw}^{wvc}$ is calculated for all measurements with wvc-averaged rain rates greater than 2 mm/hr. The mean is about -.04, indicating a slight negative bias of the weighted-average estimates. The standard deviation of the normalized error for the collocated data set is 0.39. Due to the significant variability from wvc-filling effects, the SeaWinds-derived rain rates must be interpreted as a non-uniformly weighted average of the rain rate over an area larger than the wvc, with some variance from the unweighted wvc average.

5 SIMULATIONS AND VALIDATION

Even in non-raining situations, for some wind speeds and cross track positions, the wind retrieval performance of SeaWinds is somewhat degraded.[11] This degradation often occurs at low and extreme high winds, and at nadir and on the swath edges. For low wind speeds, a low SNR often causes wind estimates to be noisy. At high wind speeds, a saturation effect in σ° occurs. On the swath edges and at nadir, poor viewing geometry causes the MLE to be ill-conditioned. However, wind retrieval is generally good at moderate wind speeds, and especially in the "sweet spot" of the swath, the off-nadir region characterized by good wind retrieval performance.

In the absence of rain, the inclusion of a rain rate parameter into the estimation process inherently makes the MLE more ill-conditioned than wind-only retrieval. However, when rain is present, the combined wind/rain retrieval can potentially significantly improve the wind estimate. It is thus important to evaluate the performance of the MLE with and without rain. Also, because the wind retrieval accuracy varies with cross-track position and wind velocity, we evaluate the performance given a variety of cross track and wind conditions.

5.1 Simulation Results

The first step in analyzing the MLE is to perform simulations of the backscatter return for various conditions and to evaluate the statistics of the retrieved wind and rain. Simulations are conducted for varying wind speeds, rain rates, wind directions and cross track positions (see Table 1). The simulation wind speeds are chosen to give a wide range of typical winds including low (3 m/s), average (7,11 m/s), high (15 m/s) and extreme (25 m/s) winds. The simulation directions cover a full 360° and are given relative to the motion of the satellite, with zero degrees pointing in the direction of flight, and angles increasing clock-wise. The simulation rain rates are logarithmically spaced covering a wide range of possible rain rates. Cross track positions are carefully chosen to provide analysis of the swath edge (wvc 6), sweet spot (wvc 14,22), and nadir (wvc 30,38) regions. Nominal values of the K_{pc} coefficients α, β, and γ are used with typical measurement geometries at each wvc.

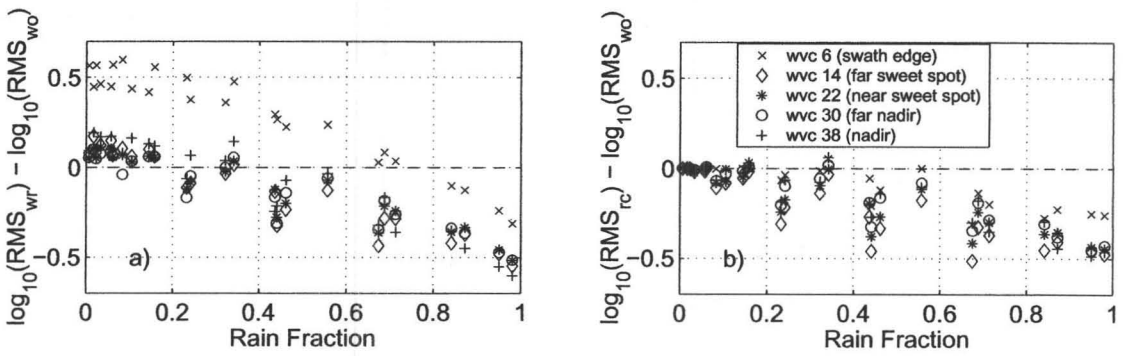

Figure 3: *Difference in normalized rms error between the a) combined wind/rain retrieval and the wind-only retrieval, and b) rain-corrected wind wind-only retrieval as a function of rain fraction.*

Table 1: *Delineations of wind speed, wind direction, rain rate, and cross track position for which the simulations are performed.*

Speed	3, 7, 11, 15, 25 m/s
Direction	0°, 15°, 30°, ..., 345°
Rain Rate	0, 0.3, 1, 3, 10, 30 mm/hr
Cross Track Position	wvc 6, 14, 22, 30, 38

For each combination of conditions, we project the speed, direction, and rain rate through the backscatter model (eq. (5)) for all measurements corresponding to that wvc. Next, we add zero-mean Gaussian random noise with the variance given in eq. (8). Retrieval is performed for 300 noise realizations for each set of conditions. The wind vector ambiguity for each realization that is closest to the true wind vector is selected.

For each simulation, 3 retrievals are performed: simultaneous wind/rain retrieval, wind-only retrieval, and rain-corrected retrieval. In simultaneous wind/rain retrieval, ambiguities are determined as the local maxima of the wind/rain likelihood function of Eq. 9. In wind-only retrieval, the baseline wind-only likelihood function of Eq. 4 is used. In rain-corrected retrieval, the simultaneous rain/wind likelihood function (Eq. 9) is evaluated at the true rain rate only, requiring *a priori* knowledge of the rain rate. Rain-corrected retrieval is like using a Beysian prior that is distributed as a delta function centered at the true rain rate, while simultaneous wind/rain retrieval is the same as using Beysian estimation with a uniform rain distribution. In the case of synergistic use of AMSR radiometer rain rates from ADEOS II, a realistic Beysian prior given the AMSR rain rates may be developed. The simulation-based rain-corrected retrieval is a "best case" scenario for a Beysian prior, whereas simultaneous wind/rain retrieval with no Beysian prior is a "worst case" scenario.

In presenting the results of the simulations, we first examine the rms error of the closest selected ambiguity to the true simulation wind as a function of cross track position and rain fraction. The rain fraction is defined as the effective rain backscatter given the rain rate divided by the total model backscatter given the retrieved rain rate and vector wind averaged over the measurements,

$$F = \sum_i \sigma_{eff}(R_i)/\mathcal{M}_r(R_i, \mathbf{u_i}, ...). \qquad (11)$$

The rain fraction indicates the level to which the rain affects the backscatter measurements. The range of wind speeds and rain rates gives a broad spectrum of rain fraction bins, each corresponding to a different wind/rain combination. To allow comparison of the wind-only retrieval to the simultaneous wind/rain and rain-corrected retrievals, the difference in rms error between each is shown in Figure 3 for each cross-track position. The logarithm of the wind only rms error (RMS_{wo}), the combined wind/rain rms error (RMS_{wr}), and the rain-corrected rms error (RMS_{rc}) is taken to improve readability of the graph. A positive difference indicates that the wind-only retrieval performs better, and a negative difference indicates that the combined wind/rain retrieval or rain-corrected retrieval performs better. Figure 3 demonstrates that combined wind/rain retrieval on the swath edge is very poor. Thus, the rest of the analysis is only performed on the inner-beam area of the swath.

From Figure 3, combined wind/rain retrieval is less accurate than wind-only retrieval for zero or low rain fraction data (corresponding to relatively low rain rates). However, for most rain fractions above 0.2, the combined rain/wind retrieval is better. The spike between 0.2 and 0.4 occurs at a wind speed of 25 m/s and rain rate of 30 mm/hr, both of which are extreme. These simulations

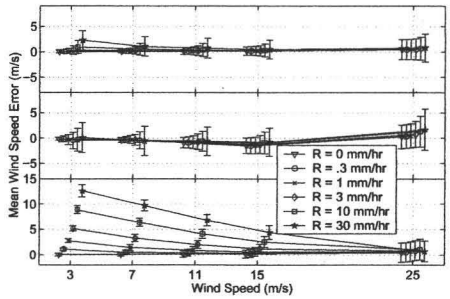

Figure 4: *Mean speed error as a function of wind speed for various rain rates. In each plot, the rain-corrected retrieval is shown on top, simultaneous wind/rain retrieval is in the middle, and wind-only retrieval is on the bottom.*

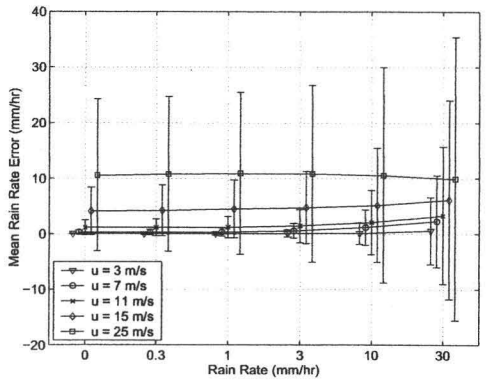

Figure 5: *Mean rain rate error as a function of rain rate for several different wind speeds.*

suggest that it is possible to improve wind estimation in many cases with no *a priori* knowledge of the rain rate.

The rain-corrected retrieval performs better than the wind-only retrieval for almost all cases. A dramatic improvement over the simultaneous retrieval is noticed on the swath edges, where simultaneous wind/rain retrieval fails. Also, as expected, the low rain fraction data performs much the same as the wind-only retrieval. For the most part, the most accurate wind retrievals are seen in the sweet spot.

The speed error for the three retrieval methods is demonstrated in Figure 4. Here all wind speeds and rain rates are shown. As expected, the wind-only retrieval shows considerable biases at low wind speeds for moderate to high rain rates. These biases are nearly completely corrected in both rain-corrected and simultaneous wind/rain retrieval which both exhibit a near-zero mean for about all cases. The rain-corrected retrieval is slightly biased high for very low rain rates and high wind speeds, while the combined wind/rain retrieved speeds are slightly biased low for most rain rate/wind speed combinations except at high wind speeds.

Next, we demonstrate the rain retrieval performance of the simultaneous wind/rain MLE. Figure 5 shows the mean rain rate error of the retrieved rain rates as a function of true rain rate for varying wind speeds. As wind speed increases, the MLE becomes increasingly biased. The rain rate bias at high wind speeds is quite high, even at zero rain rate. This suggests that at high wind speeds, ambiguities with spurious rain rates may exist. However, in low to moderate wind speeds (3-11 m/s), the retrieval performs quite well. This simulations demonstrates the limitation of accurately retrieving rain in high wind speed regions. Rain flagging algorithms can be developed to detect erroneous rain rates in high wind speed regions and discard them.

5.2 Validation

In this section, we present a validation of QuikSCAT simultaneous wind/rain retrieval to TRMM PR rain rates. A scatter plot of the PR rain rates against the QuikSCAT rain rates are shown in Figure 6. Although the QuikSCAT derived rain rates have considerable scatter in comparison to the PR rain rates, Figure 6 demonstrates that there is definately a strong correllation between the QuikSCAT and PR-derived rain rates. The QuikSCAT rain rates are somewhat biased high, which is expected from simulation. However, the bias can be corrected.

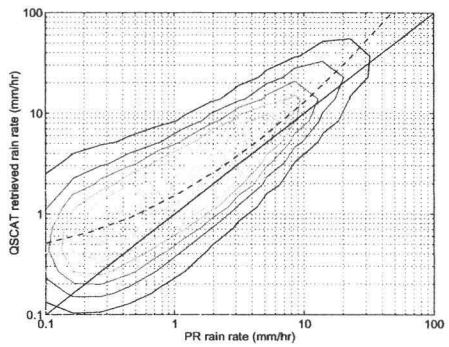

Figure 6: *Scatter plot of TRMM PR rain rates versus QuikSCAT rain rates. Density curves are shown, along with the equality line (solid). The dotted line represents the best quadratic fit of PR rain rate to QSCAT rain rate (in log space).*

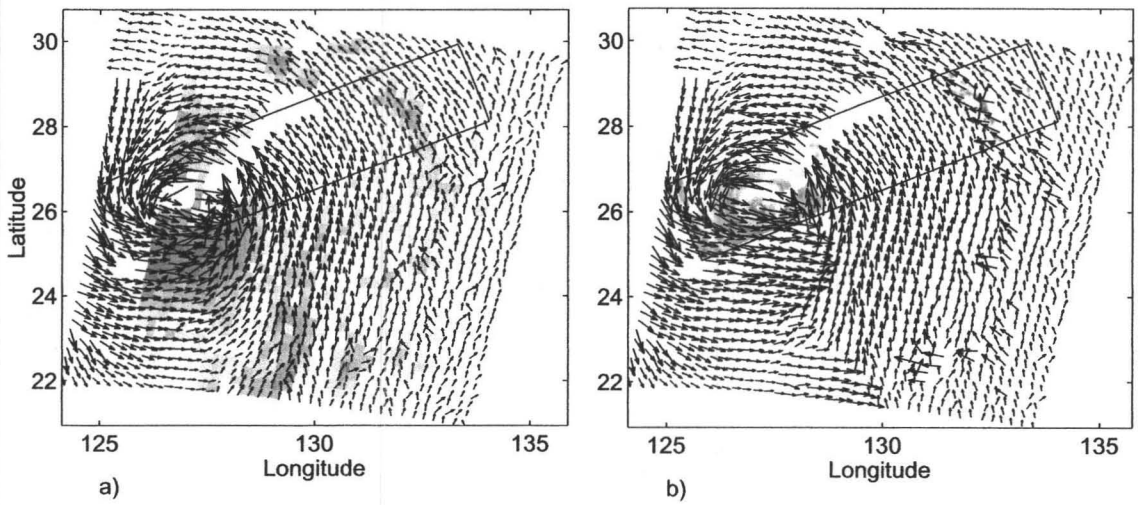

Figure 7: *Synoptic example of a storm with a) simultaneous wind/rain retrieval; QuikSCAT-derived rain rate is shown in the background and b) wind-only retrieval; TRMM PR-derived rain rates are shown in the background. The grayscale shades range from .1 to 100 mm/hr rain rates. The box shows the coverage of the PR data*

6 SYNOPTIC EXAMPLE

In this section, we examine a collocated PR/QuikSCAT example over a hurricane. The location of the storm is over the Ryukyu Islands off the southern tip of Japan on September 22, 1999. Figure 7 shows the QuikSCAT-derived wind vectors for both simultaneous wind/rain and wind-only retrieval, along with the QuikSCAT-derived rain rates and the collocated TRMM PR derived rain rates.

On the far right of the figure, the coverage of the storm is limited to the outer-beam region of the QuikSCAT swath. Thus, retrieval of rain in this area is not possible. Instead, the wind-only retrieved solutions are shown for the Figure 7a on the swath edge.

The wind-only retrieval exhibits many rain-induced features that are corrected by the simultaneous wind/rain retrieval. The most obvious of these features are the rain bands located up to about 24 wind vector cells (600 km) from the center of the storm. The rain band is also visible in the TRMM PR data. The wind-only retrieval shows dramatic "apparent" wind speed increases and corrupted directions due to the electromagnetic scattering from the rain. The simultaneous wind/rain retrieval nearly shows wind speeds in the rain bands that are much closer to the actual wind speeds of neighboring wvcs, with somewhat more self-consistent directions for the most part.

Another rain feature that the simultaneous wind/rain retrieval corrects is the corruption due to the large area of rain just south of the storm center. In this case, the wind-only retrieval shows wind vectors all pointing nearly east (in the cross-track direction), which is an indicator of rain. The QuikSCAT-retrieved rain rates are very high in this region, which is consistent with the QuikSCAT retrieved rains over portion covered by the PR. The simultaneous wind/rain retrieval shows a much more consistent circular flow in this region, suggesting better wind retrieval over the wind-only method. These corrected features demonstrate that the simultaneous wind/rain retrieval has the capability of correcting rain-corrupted winds.

7 CONCLUSIONS

QuikSCAT is a spaceborne scatterometer, originally designed to measure ocean winds. Rain has been shown to be one of the most significant factors that corrupts wind scatterometer data. However, a new technique of simultaneously retrieving ocean winds and rain has been can significantly improve the wind estimate for most rain-corrupted areas. As a side benefit, the simultaneous wind/rain retrieval gives an estimate of the rain rate, which is somewhat noisy, but has much larger coverage than instruments such as the TRMM PR.

SeaWinds on QuikSCAT rain retrieval has been shown by simulation to give the best results in the sweet spot, and to not work well on the swath edges. However, the swath edges are observed from v-pol only, which less sensitive to rain than the inner-beam h-pol data.

Simulation also demonstrates that wind speeds from simultaneous wind/rain retrieval are nearly unbiased, while the wind-only retrieval produces increasingly bi-

ased estimates as rain fractions increase. However, at low rain fractions, the simultaneous wind/rain retrieval is more ill conditioned, and thus does not perform as well as wind-only retrieval in these areas. Thus it is beneficial to develop a rain flag, and only perform simultaneous retrieval in raining areas.

Future research includes further refining of K_{pe}, the development of a rain flag using the simultaneously wind rain retrieval, and further analysis of the QuikSCAT-derived rain rates as a function of cross-track and global position.

References

[1] M. W. Spencer, C. Wu, and D. G. Long, "Tradeoffs in the design of a spaceborne scanning pencil beam scatterometer: Application to SeaWinds," *IEEE Trans. Geosci. Rem. Sens.*, vol. 35, pp. 115–126, 1997.

[2] C. Chi and F. K. Li, "Comparative study of several wind estimation algorithms for spaceborne scatterometers," *IEEE Trans. Geosci. Rem. Sens.*, vol. 26, pp. 115–121, 1988.

[3] B. W. Stiles and S. Yueh, "Impact of rain on spaceborne Ku-band wind scatterometer data," *IEEE Trans. Geosci. Rem. Sens.*, vol. 40, no. 9, pp. 1973–1983, 2002.

[4] J. N. Huddleston and B. W. Stiles, "A multi-dimensional histogram rain flagging technique for SeaWinds on QuikSCAT," in *IGARSS 2000.* IEEE International Geoscience and Remote Sensing Symposium, July 24-28 2000, pp. 1232–1234.

[5] M. H. Freilich and R. S. Dunbar, "Derivation of satellite wind model functions using operational surface wind analyses - an altimeter example," *J. Geophys. Res.*, vol. 98, no. C8, pp. 14,633–14,649, Aug 15 1993.

[6] B. W. Stiles, B. D. Pollard, and R. S. Dunbar, "Direction interval retrieval with thresholded nudging: A method for improving the accuracy of QuikSCAT winds," *IEEE Trans. Geosci. Rem. Sens.*, vol. 40, pp. 79–89, 2002.

[7] David G. Long and Michael W. Spencer, "Radar backscatter measurement accuracy for a spaceborne pencil-beam wind scatterometer with transmit modulation," *IEEE Trans. Geosci. Rem. Sens.*, vol. 35, no. 1, pp. 102–114, Jan 1997.

[8] T. E. Oliphant and D. G. Long, "Accuracy of scatterometer derived winds using the Cramér-Rao bound," *IEEE Trans. Geosci. Rem. Sens.*, vol. 37, pp. 2642–2652, 1999.

[9] S. J. Shaffer, R. S. Dunbar, S. V. Hsiao, and D. G. Long, "A median-filter-based ambiguity removal algorithm for NSCAT," *IEEE Trans. Geosci. Rem. Sens.*, vol. 29, pp. 167–174, 1991.

[10] D. W. Draper and D. G. Long, "Evaluating the effect of rain on seawinds scatterometer measurements," in review, 2003.

[11] D. W. Draper and D. G. Long, "An assessment of SeaWinds on QuikSCAT wind retrieval," to appear, 2002.